Available online at www.sciencedirect.com
SCIENCE DIRECT®
Fluid Phase Equilibria 224 (2004) 237–244
FLUID PHASE EQUILIBRIA
www.elsevier.com/locate/fluid

Solid deposition as a function of temperature in the nC_{10} + (nC_{24}–nC_{25}–nC_{26}) system

Jérôme Pauly[a], Jean-Luc Daridon[a,*], Joao A.P. Coutinho[b]

[a] *Laboratoire des Fluides Complexes–Groupe Haute Pression, Université de Pau, BP 1155, 64013 PAU Cedex, France*
[b] *CICECO, Departamento de Quimica da Universidade de Aveiro, 3810-193 Aveiro, Portugal*

Received 24 January 2004; accepted 18 June 2004

Abstract

The amount and composition of wax precipitation were determined as a function of temperature below the wax appearance temperature in the synthetic system decane + (tetracosane–pentacosane–hexacosane). Measurements were performed by filtration and chromatographic analysis of the partially frozen mixtures. Wax contents were obtained from mass balance after correction of the entrapped liquid in the solid residue. Experimental results were compared with the values calculated by various predictive models.

Keywords: liquid–Solid equilibrium; Wax; Paraffin

1. Introduction

Petroleum reservoir fluids like heavy oils or gas condensate contain high-molecular weight hydrocarbons, which may precipitate as a waxy solid-phase when conditions of temperature and pressure change during production and transport. Wax deposition on the walls of the production equipment or along flow-lines reduces the diameter of the tubing and may obstruct it completely, if it is not prevented. This process results from changes of both temperature condition and fluid composition during the production. In order to prevent this phenomenon, it is essential to be able to predict, by the use of thermodynamic models, the wax appearance temperature (WAT) as well the behavior of the solid waxy phase below WAT.

To develop and test the reliability of such models, it is important to obtain experimental data of liquid–solid equilibrium for systems with a well known composition. With this objective, measurements of liquid–solid equilibrium on synthetic mixtures have been undertaken. The composition of the studied systems represents a highly simplified model of a crude oil. Thus, five different samples made up of a solvent (decane) and a heavy fraction with three consecutive normal paraffins (C_{24}–C_{25}–C_{26}) have been investigated. Only the paraffin distribution of the heavy fraction is changed in the five systems, in order to test its influence on liquid–solid equilibrium. Measurements were performed by phase separation in a filtration cell under atmospheric pressure at temperatures ranging from the WAT to the point where 90% of the heavy fraction is precipitated.

The experimental data were then compared with those predicted by two different thermodynamic models [1,2]. The first model is the one developed by Coutinho et al. [1], specifically for the description of wax formation at atmospheric pressure, whereas the second one is the model developed previously by Pauly et al. [2], valid for a much larger range of pressures.

2. Experimental technique

The method generally used to characterize phase equilibrium between fluid phases consists of taking and analyzing a micro-sample of each of the phases present in equilibrium

* Corresponding author. Tel.: +33 5 59 92 30 54; fax: +33 5 59 40 76 95.
E-mail address: jean-luc.daridon@univ-pau.fr (J.-L. Daridon).

0378-3812/$ – see front matter © 2004 Elsevier B.V. All rights reserved.
doi:10.1016/j.fluid.2004.06.057

for all the temperatures investigated. Unfortunately, in the case of liquid–solid equilibrium, where the solid-phase is made up of an aggregation of crystals, which are not necessarily homogeneous and retains important quantities of fluid, sampling cannot be considered as representative of the composition of the solid-phase. In this situation, to accurately determine the composition of the solid-phase, it has to be purged as much as possible from the entrapped liquid and then analyzed as a whole. To do this, we selected the following procedure.

The phase separation, obtained from compression of the system through a filter of 2 μm porosity, is performed in a transparent cell equipped with a moving piston at the first end and a filtering system coupled to an autoclave valve at the other one [3]. This porosity is acceptable for the kind of systems in which large crystals are observed, as in Fig. 1.

When the filtration is completed, the two recovered phases are weighed and then analyzed using gas chromatography on a Hewlett-Packard 6890 chromatograph equipped with an on-column injector and a 60 × 0.32 mm^2 Ohio Valley OV-50.5 μm capillary, with a temperature program of 3 °C/min from 50 °C to 320 °C. Based on precise knowledge of the total mass of the sample and the quantity of matter present in the two phases, we were able to estimate, by means of a material balance, that the total quantity of chemicals retained in the filtration system and valve, and on the cell walls was less than 1% for all the tests performed.

At this stage, only the composition of the liquid phase is determined accurately. The solid-phase, which is made up of a myriad of crystals, tends to entrap part of the liquid in the crystals after filtration. The filtration residue corresponds to a mixture of the solid-phase and of trapped liquid. Given the nature of the systems studied, which are made up of a pure solvent, which is much lighter than the heavy fraction, the proportion of liquid trapped in the solid-phase can be determined easily from the quantity of solvent measured in the solid residue. Because the difference in chain length between decane and the first distribution paraffin is substantial (13 carbons), there cannot be any partial miscibility between the heavy paraffins and decane according to the Kravchenko rule [4]. As the melting temperature of the solvent is 243 K, it may not crystallize in the range of temperatures investigated. Its presence in the solid-phase is assumed to be due to the existence of the trapped liquid. In order to prove this assumption, we have performed a filtration experiment with an internal standard (about 5% of toluene) whose melting temperature is sufficiently lower than those of decane. The analysis of liquid and solid residue shows the same ratio of toluene/decane in both parts (with a deviation less than 0.15%). Thus, this result clearly demonstrates that the presence of solvent in the solid residue is due to entrapped liquid and not solid-phase.

As the exact composition of the liquid phase is known from chromatography, it is possible to calculate the total amount of entrapped liquid by:

$$X^{\mathrm{el}} = \frac{X^{\mathrm{sr}}_{\mathrm{solvent}}}{X^{\mathrm{l}}_{\mathrm{solvent}}} \tag{1}$$

in which $X^{\mathrm{sr}}_{\mathrm{solvent}}$ and $X^{\mathrm{l}}_{\mathrm{solvent}}$ correspond to the mass fraction of solvent analyzed in two parts recovered after filtration. The quantity of solid crystallized (expressed in mass fraction) can thus be corrected by:

$$X^{\mathrm{s}} = X^{\mathrm{sr}}(1 - X^{\mathrm{el}}) \tag{2}$$

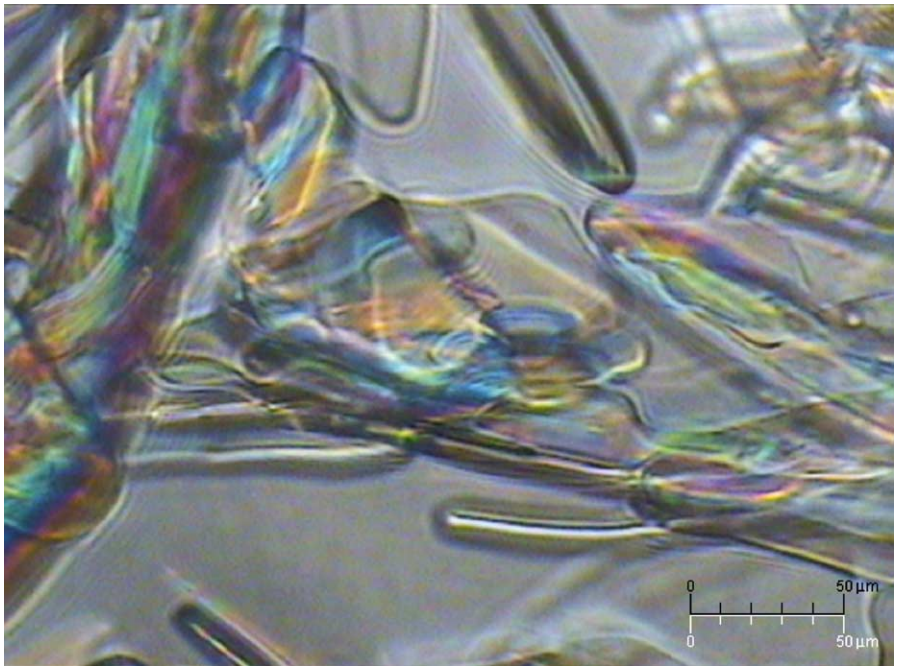

Fig. 1. Photo of liquid–solid equilibrium for the C_{10}+(C_{24}–C_{25}–C_{26}) system (obtained by microscopy).

The real composition of the solid-phase is then given by:

$$X_i^s = \frac{(X_i^{sr} - X^{el} X_i^l)}{(1 - X^{el})} \quad (3)$$

for any component i of the heavy fraction. The proportion of entrapped liquid proved to be constant (about 5%) in the solid residue (X^{el}) for all the studied compositions in the overall range of investigated temperatures. This invariability indicates the lack of thermodynamic phenomenon related to the decane presence in the solid-phase and shows that the entrapped liquid existence is inherent to the separation process.

3. Measurements

Measurements have been carried on five mixtures with different composition of the system nC_{10}+(nC_{24}–nC_{25}–nC_{26}). All the investigated mixtures have been prepared with Aldrich or Fluka products (with a purity degree >99%) in order to obtain a global molar composition between the solvent and the heavy fraction identical in the five systems (80% of nC_{10} + 20% of heavy fraction). Only the composition of the compounds present in the heavy fraction differs from one sample to the other as described in Table 1.

These heavy components, which are chosen in the linear alkane family, have been distributed within the heavy fraction following the relationship:

$$x_{C_{n+1}} = \alpha . x_{C_n} \quad (4)$$

corresponding to a simplified representation of the heavy fraction found in paraffinic crudes when the α parameter is close to 0.8. In this work, we have considered different values of the α coefficient (Table 1) in order to study the influence of the heavy component distribution within the global composition on the precipitation and, in particular, on the physico-chemical composition close to the WAT. The following three cases have been considered:

- $\alpha < 1$ characterizes a decreasing distribution and then represents the repartition observed in crude oils;
- $\alpha = 1$ rendering an equimolar repartition of the heavy paraffins; and
- $\alpha > 1$ corresponding to increase of the molar number with the carbon number of the molecule. This assumption defines a behavior opposed to the real fluid behavior.

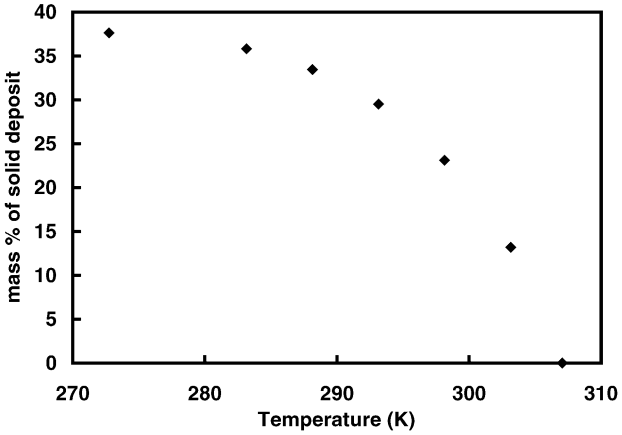

Fig. 2. Influence of T on solid deposit for mixture 5.

Measurements were carried out every 3 or 4 K from the phase change temperature to the temperature where 90% of the paraffins are crystallized. The amount of solid deposit versus temperature are reported in Tables 2–6 and plotted, for example, in Fig. 2. In these tables, the solid-phase compositions are also recorded. From the results obtained on the quantities and compositions of the phases present in equilibrium, it is possible to express the percentage of crystallized paraffins. These data are given in Tables 2–6 that display the overall percentage of paraffins crystallized, as well as the percentages corresponding to the individual crystallized paraffins. Their evolutions, as a function of temperature, are illustrated in Fig. 3.

The C_{24}-C_{25}-C_{26} paraffin distribution within the solid-phase is schematized in the Figs. 4 and 5, which correspond, respectively, to the mixtures 1 and 5. These diagrams show clearly three different tendencies:

- the proportion of the lightest component of the heavy fraction increases with decreasing temperature;
- the reversed tendency is observed for the heaviest one; and
- finally the composition of the intermediate component does not seem to be affected by the temperature.

The experimental data allows estimation, in all phases, of the distribution factor α between the heavy components versus temperature. This parameter is no more constant, meaning that the repartition of compounds in heavy fraction is no more described by the Eq. (4). The distribution factors in

Table 1
Overall characteristics of the investigated systems

		Mixture 1	Mixture 2	Mixture 3	Mixture 4	Mixture 5
Overall composition (molar %)	n-C_{10}	79.99	80.00	80.01	80.00	80.00
	Heavy fraction	20.01	20.00	19.99	20.00	20.00
Heavy fraction distribution (molar %)	n-C_{24}	51.01	38.55	33.35	26.24	21.06
	n-C_{25}	30.60	33.08	33.33	32.78	31.58
	n-C_{26}	18.39	28.38	33.32	40.98	47.36
	α	0.600	0.858	1.00	1.25	1.50
	MW (g/mol)	348.11	351.26	352.68	354.75	356.37

Table 2
Quantity and composition of the solid deposit in mixture 1

		301.15 K	297.25 K	293.15 K	288.25 K	283.15 K	278.15 K
Solid deposit (mass %)		12.94	21.31	27.61	31.36	32.96	35.3
Solid-phase composition (mass %)	C_{24}	40.65	42.47	44.37	46.78	47.65	48.5
	C_{25}	34.34	33.67	33.08	32.15	31.7	31.29
	C_{26}	25.01	23.86	22.55	21.07	20.65	20.22
Crystallized paraffins (mass %)	Total	34.56	56.3	72.39	83.85	90.61	94.83
	C_{24}	28.26	48.1	64.78	78.93	87.51	92.86
	C_{25}	38.71	61.93	78.06	87.98	93.24	96.57
	C_{26}	44.01	68.53	82.7	89.87	94.24	97.07

Table 3
Quantity and composition of the solid deposit in mixture 2

		302.25 K	299.55 K	296.55 K	294.45 K	292.65 K
Solid deposit (mass %)		12.72	21.56	25.95	27.04	29.01
Solid-phase composition (mass %)	C_{24}	26.70	29.10	30.32	31.86	32.76
	C_{25}	34.67	34.65	34.40	34.08	34.17
	C_{26}	38.63	36.25	35.27	34.06	33.07
Crystallized paraffins (mass %)	Total	29.62	52.00	64.01	72.00	77.14
	C_{24}	21.08	40.01	51.84	61.79	68.27
	C_{25}	31.60	55.73	68.11	75.91	80.89
	C_{26}	38.19	63.12	74.70	80.26	83.91

Table 4
Quantity and composition of the solid deposit in mixture 3

		301.15 K	297.15 K	293.15 K	289.15 K	285.15 K	281.15 K
Solid deposit (mass %)		15.24	22.55	27.46	31.69	33.96	34.39
Solid-phase composition (mass %)	C_{24}	22.83	24.86	26.95	28.43	29.64	30.45
	C_{25}	33.96	34.27	34.26	33.99	33.68	33.47
	C_{26}	43.21	40.87	38.80	37.58	36.67	36.08
Crystallized paraffins (mass %)	Total	41.86	62.31	75.32	83.99	89.76	93.67
	C_{24}	29.7	48.35	63.31	74.61	83.04	88.95
	C_{25}	43.27	64.84	78.43	86.79	91.96	95.3
	C_{26}	51.73	72.7	83.39	89.91	93.87	96.45

Table 5
Quantity and composition of the solid deposit in mixture 4

		301.15 K	297.95 K	293.05 K	288.15 K	283.05 K	278.15 K
Solid deposit (mass %)		16.97	22.59	27.71	31.04	34.43	36.15
Solid-phase composition (mass %)	C_{24}	17.22	18.05	19.83	21.77	23.26	24.27
	C_{25}	32.12	32.34	32.78	32.93	32.79	32.64
	C_{26}	50.66	49.61	47.39	45.29	43.94	43.10
Crystallized paraffins (mass %)	Total	51.8	67.68	86.75	89.33	94.98	97.11
	C_{24}	36.52	50.9	75.05	79.02	89.36	93.62
	C_{25}	51.61	67.93	87.67	90.83	96.07	97.9
	C_{26}	60.55	76.6	92.09	94.09	97.39	98.57

Table 6
Quantity and composition of the solid deposit in mixture 5

		303.15 K	298.15 K	293.15 K	288.15 K	283.15 K	272.75 K
Solid deposit (mass %)		13.18	23.11	29.52	33.46	35.83	37.63
Solid-phase composition (mass %)	C_{24}	12.32	13.55	14.83	16.30	17.61	19.16
	C_{25}	29.29	30.06	30.62	31.05	31.18	31.04
	C_{26}	58.38	56.40	54.55	52.65	51.21	49.80
Crystallized paraffins (mass %)	Total	38.62	62.19	78.84	87.8	93.14	97.97
	C_{24}	23.76	41.83	59.32	72.57	82.83	94.21
	C_{25}	36.72	60.61	78.38	88.45	94.15	98.57
	C_{26}	45.84	71.56	86.9	93.43	96.65	99.12

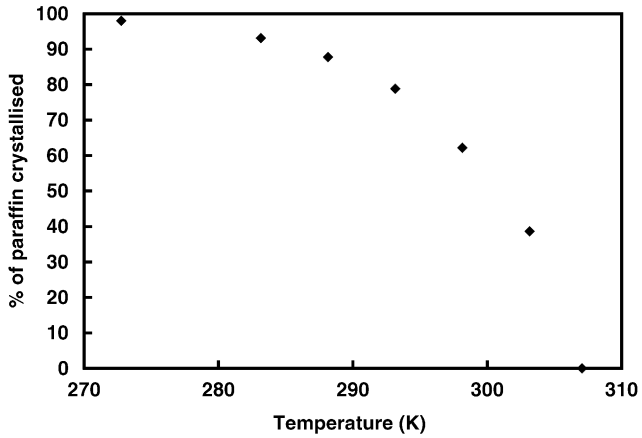

Fig. 3. Percentage (mass) of paraffins crystallised vs. T (mixture 5).

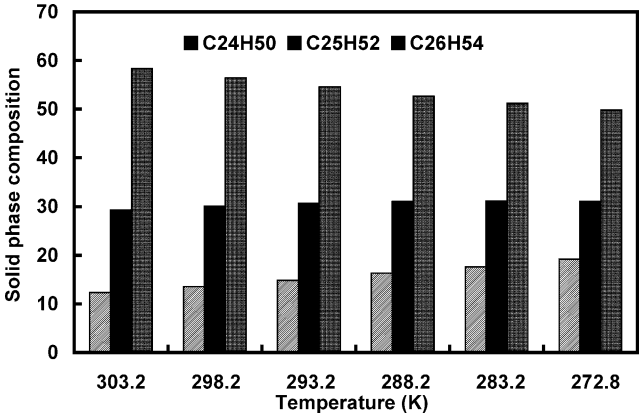

Fig. 5. Solid-phase composition as a function of T (mixture 5).

solid-phase are always larger than the α coefficients in the global composition. For the highest temperature, the coefficient between C_{24} and C_{25} is always about 1.4–1.5 times α_{global}, whereas between C_{25} and C_{26}, it is approximately 1.2 or 1.3 times α_{global} for all the investigated systems. This remark, which is valid for all the mixtures, means that the proportion of C_{26} becomes significant in the solid-phase compared with the overall composition. When the temperature decreases below the WAT, distribution factors drop (Fig. 6) to reach the initial composition where 100% of the paraffins have crystallized.

4. Modeling

Experimental data were compared to the predictions of two models [1,2] based on the same representation of the solid-phase but using different approach to describe the non-ideality in the liquid phase. The first one, proposed by Coutinho et al. [1], rests on Flory free-volume equation [5,6] to represent the entropic effects, such as size difference and free-volume effects. The activity coefficient is then expressed by the equation:

$$\ln \gamma_i^{comb+fv} = \ln \frac{\phi_i}{x_i} + 1 - \frac{\phi_i}{x_i} \quad (5)$$

with

$$\phi_i = \frac{x_i (V_i^{1/3} - V_{wi}^{1/3})^{3.3}}{\sum_j x_j (V_j^{1/3} - V_{wj}^{1/3})^{3.3}} \quad (6)$$

where V_i is the molar volume and V_{wi} is the van der Waals volume of the component i.

This model was chosen here as it was shown [3] from tests performed with several models [7–11] that this approach leads to a satisfactory representation of the liquid–solid equilibrium of the multi-paraffins systems. However, this model, which is based on excess Gibbs free energy models, is restricted to low pressures. In order to extend the Coutinho-type

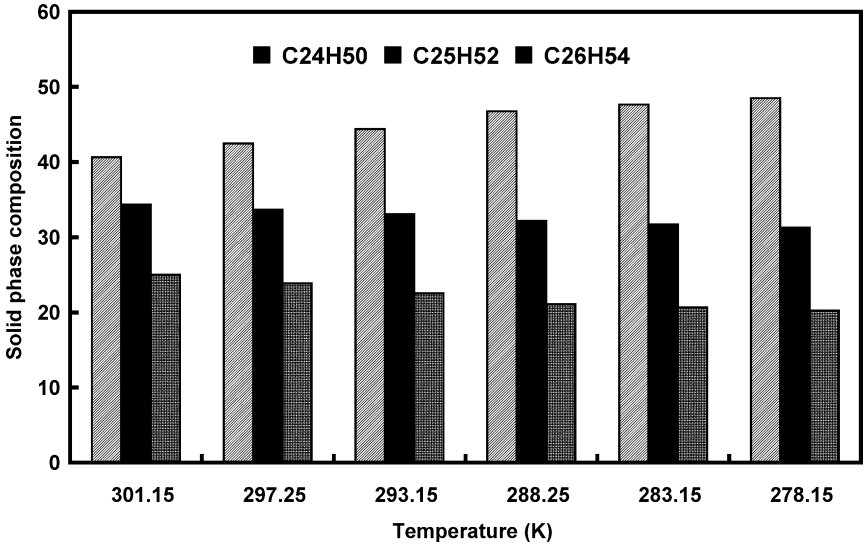

Fig. 4. Solid-phase composition as a function of T (mixture 1).

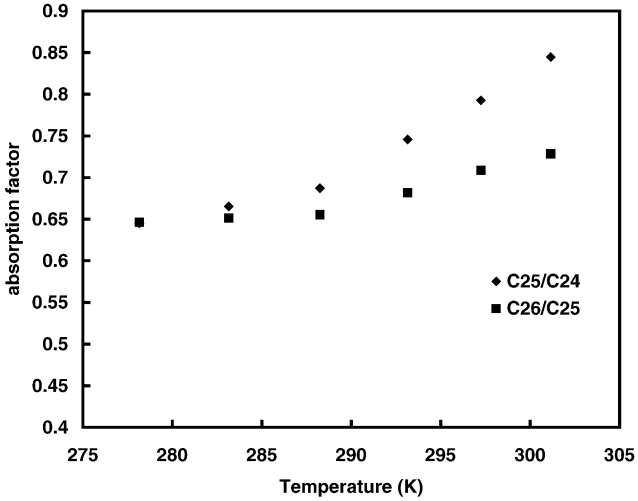

Fig. 6. Evolution of the distribution factors C_{25}/C_{24} and C_{26}/C_{25} (mass) vs. T (mixture 1).

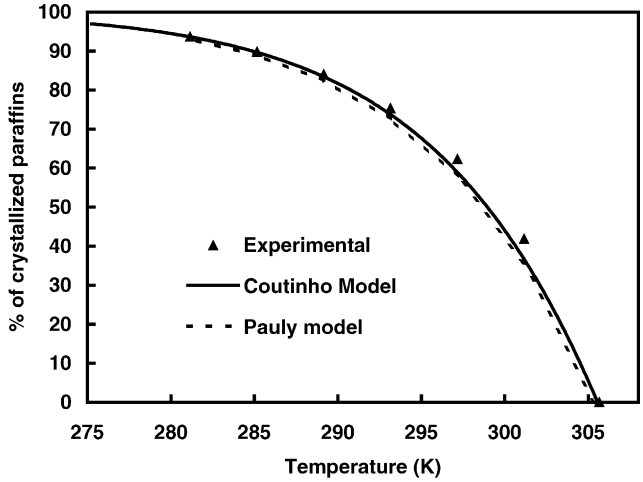

Fig. 7. Comparison between the experimental and calculated percentage of crystallized paraffins (mixture 3).

model to a broad range of pressures, Pauly et al. [2] proposed using a cubic equation of state (Soave [12]) with a g^E mixing rule (LCVM [13]) model to describe the fluid phase behavior under pressure. This second model tested use the modified UNIFAC group contribution method [14] with interaction parameters in the following form [9,15]:

$$\Psi_{ij} = \exp\left(-\frac{A_{ij} + B_{ij}(T - 298.15)}{T}\right) \tag{7}$$

to evaluate the Gibbs free energy in the mixing rule.

According to width of the distribution of paraffins and the work of Craig et al. [16], Dirand et al. [17], Chevallier et al. [18,19] and Gerson et al. [20,21], the solid-phase was assumed as a single orthorhombic solid solution. The non-ideality of this solid solution was described in both models by a predictive version of the local composition model of Wilson [22] where local mole fractions are employed instead of local volumetric fractions as proposed by Coutinho et al. [1]:

$$\frac{g^E}{RT} = -x_l \ln\left(x_l + x_s \exp\left(-\frac{\lambda_{ls} - \lambda_{ll}}{RT}\right)\right)$$

$$-x_s \ln\left(x_s + x_l \exp\left(-\frac{\lambda_{ls} - \lambda_{ss}}{RT}\right)\right) \tag{8}$$

where "l" and "s" represent the long and the short molecule, respectively. The pair interaction energies, λ_{ij}, are related to the coordination number, $Z = 6$, and to the enthalpy of sublimation of pure alkanes:

$$\lambda_{ij} = \lambda_{ii} \quad \text{and} \quad \lambda_{ii} = -\frac{2}{Z}(\Delta h_{sbl} - RT) \tag{9}$$

where i is the *n*-alkane with the shorter chain of the pair ij.

To appreciate the respective abilities of these models to predict the L–S transition temperatures, the deviations between the calculated and the experimental values are listed in Table 7. The deviations observed with the model proposed by Coutinho et al. [1] are for the five systems less than 0.5 K. This performance is all the more remarkable as the model is used in its original form, in other words, without any adjustment of parameters.

In the same way, the approach proposed by Pauly et al. [2], produces a very good estimation of the WAT (less than 0.8 K) without systematic deviation. These results are not surprising, since the approach of Pauly et al. is an extension to high pressure of the model of Coutinho. Thus, at atmospheric

Table 7
WAT Deviation ΔT for the two tested models

		Mixture 1	Mixture 2	Mixture 3	Mixture 4	Mixture 5
WAT_{exp}/K		303.35	304.95	305.65	306.15	307.05
ΔT/K	Coutinho et al. [1]	+0.5	+0.1	−0.1	+0.2	−0.1
	Pauly et al. [2]	+0.8	0.0	−0.3	−0.1	−0.5

Table 8
Absolute average deviation (%) between the experimental and calculated solid deposit quantity

	Mixture 1	Mixture 2	Mixture 3	Mixture 4	Mixture 5
Coutinho et al. [1]	5.4	9.1	3.5	8.7	3.5
Pauly et al.	5.3	10.0	4.8	10.0	6.1

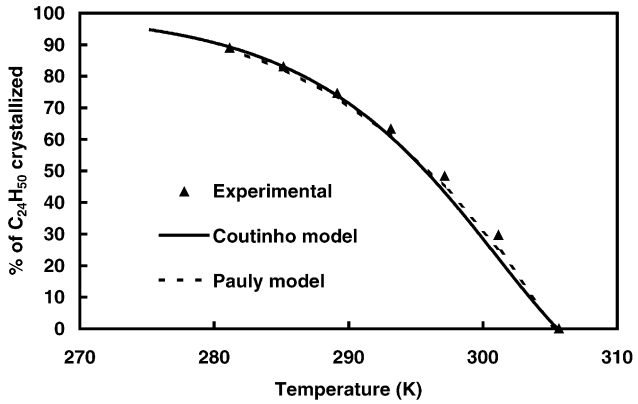

Fig. 8. Comparison between the experimental and calculated percentage of $C_{24}H_{50}$ crystallized (mixture 3).

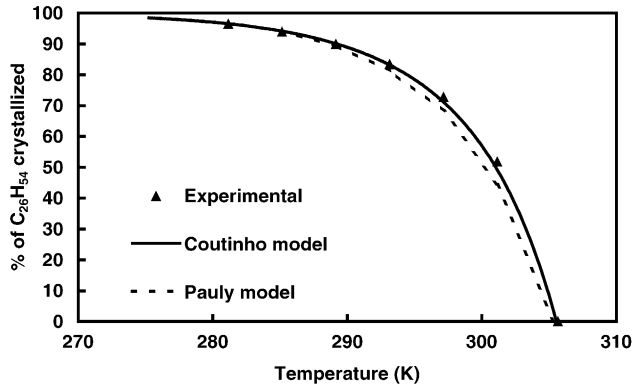

Fig. 9. Comparison between the experimental and calculated percentage of $C_{26}H_{54}$ crystallized (mixture 3).

pressure the only difference between the two models is the g^E model used to describe the non-ideality of the liquid phase.

In Table 8, the predicted percentage of paraffin crystallized is compared successfully with the experimental results from the two approaches. The absolute average deviations never exceed 10% for the five investigated mixtures. In Fig. 7, where the same kind of results are represented for the mixture 3, a decrease in temperature leads to an increase of the solid deposit and the predictions are very accurate in all the range of studied temperatures.

In order to test the capability of the models, to predict the behavior of each paraffin individually, the percentage of crystallization of both lightest and heaviest paraffin are represented in Figs. 8 and 9, respectively. The modeling results from the two approaches are very similar and in excellent agreement with experimental data. Actually, the results can be extended to the five mixtures demonstrating that the assumption of the heavy components precipitation in one solid solution seems to be correct [3].

5. Conclusion

In spite of the intense interest that characterises the petroleum fluids, it turns out that important gaps remain in the experimental heavy fractions characterisation. In particular, only a very few data are available in the literature concerning the behavior of the solid fraction versus pressure and temperature.

Thus, experimental equipment of solid–liquid filtration and measurement procedure has been developed in order to study the solid precipitation in synthetic mixtures. The apparatus was used to perform experimental measurements on mixtures made up of decane plus various distributions of heavy normal paraffins from tetracosane to hexacosane. These measures concern the amount and the composition of solid precipitate as a function of temperature on synthetic complex systems as well as the cloud point temperature at atmospheric pressure. The modeling performed on the data measured on this work demonstrates that the procedure proposed by Coutinho et al. [1] as well the model by Pauly et al. [2] leads to a good description of the liquid–solid equilibrium of these multi-component systems.

List of symbols:

g	Gibbs free energy
h	enthalpy
P	pressure
R	ideal gas constant
T	temperature
V	volume
x	mole fraction
Z	coordination number

Greek letters:

ϕ	fugacity coefficient
γ	activity coefficient
λ	interaction parameters of Wilson equation
Ψ	interaction parameters of UNIFAC

Superscripts:

E	Excess
el	entrapped liquid
l	liquid
s	solid
sr	solid residue

Subscripts

i	component
cn	carbon number
l	long
s	short
sbl	sublimation

References

[1] J.A.P. Coutinho, K. Knudsen, S.I. Andersen, E.H. Stenby, Chem. Eng. Sci. 51 (1996) 3273–3282.
[2] J. Pauly, J.L. Daridon, J.A.P. Coutinho, N. Lindeloff, S.I. Andersen, Fluid Phase Equilib. 167 (2000) 145–159.
[3] J. Pauly, C. Dauphin, J.L. Daridon, Fluid Phase Equilib. 149 (1998) 191–207.

[4] V. Kravchenko, Acta Physicochim. 21 (1946) 335.
[5] P.J. Flory, Thermodynamics of polymer solutions, Discuss. Faraday Soc. 49 (1970) 7–29.
[6] T. Oishi, J.M. Prausnitz, Ind. Eng. Chem. Process Des. Dev. 17 (1978) 333–339.
[7] J.A.P. Coutinho, S.I. Andersen, E.H. Stenby, Fluid Phase Equilib. 103 (1995) 23–39.
[8] K.W. Won, Fluid Phase Equilib. 30 (1986) 265.
[9] J.H. Hansen, A. Fredenslund, K.S. Pedersen, H.P. RØnningsen, AIChE J. 34 (1988) 1937.
[10] P. Ungerer, B. Faissat, C. Leibovici, H. Zhou, E. Behar, Fluid Phase Equilib. 111 (1995) 287.
[11] K.S. Pedersen, P. Skovborg, H.P. RØnningsen, Energy Fuels 5 (1991) 924.
[12] G. Soave, Chem. Eng. Sci. 27 (1972) 1197–1203.
[13] C.J. Boukouvalas, N. Spiliotis, N. Ph Coustikos, D.P. Tzouvaras, Tassios, Fluid Phase Equilib. 92 (1994) 75.
[14] B.L. Larsen, P. Rasmussen, A. Fredenslund, Ind. Eng. Chem. Res. 26 (1987) 2274.
[15] C.J. Boukouvalas, K.G. Magoulas, S.K. Stamataki, D. Tassios, Ind. Eng. Chem. Res. 36 (1997) 5454.
[16] S.R. Craig, G.P. Hastie, K.J. Roberts, A.R. Gerson, J.N. Sherwood, R.D. Tack, J. Mater. Chem. 8 (1998) 859–869.
[17] M. Dirand, V. Chevallier, E. Provost, M. Bouroukba, D. Petitjean, Fuel 77 (12) (1998) 1253–1260.
[18] V. Chevallier, E. Provost, J.B. Bourdet, M. Bouroukba, D. Petitjean, M. Dirand, Polymer 40 (1999) 2121–2128.
[19] V. Chevallier, D. Petitjean, M. Bouroukba, M. Dirand, Polymer 40 (1999) 2129–2137.
[20] AR. Gerson, K.J. Roberts, J.N. Sherwood, Am. Inst. Chem. Eng. Symp. Ser. 284 (1991) 138–142.
[21] AR. Gerson, K.J. Roberts, J.N. Sherwood, J.N. Taggart, G. Jackson, J. Crystal Growth 128 (1993) 1176–1181.
[22] G.M. Wilson, J. Am. Chem. Soc. 86 (1964) 127.